Journal of Alloys and Compounds 622 (2015) 362–368

Contents lists available at ScienceDirect

Journal of Alloys and Compounds

journal homepage: www.elsevier.com/locate/jalcom

Temperature-stable and high Q composite ceramics in low-temperature sinterable $BaO–V_2O_5$ binary system

Chen Zhang, Ruzhong Zuo *

Institute of Electro Ceramics & Devices, School of Materials Science and Engineering, Hefei University of Technology, Hefei 230009, PR China

ARTICLE INFO

Article history:
Received 30 May 2014
Received in revised form 17 September 2014
Accepted 11 October 2014
Available online 23 October 2014

Keywords:
High Q
Near-zero τ_f
Microwave dielectric properties
LTCC

ABSTRACT

The low-temperature sinterable microwave dielectric composites with compositions of $(1-x)Ba_2V_2O_7–xBa_3(VO_4)_2$ ($x = 0.27–0.52$, in volume fraction) were prepared by cofiring mixtures of pure-phase $Ba_2V_2O_7$ and $Ba_3(VO_4)_2$. The phase structure and grain morphology of the ceramics were studied by X-ray diffraction and field emission scanning electron microscopy. The results indicated that the two phases of $Ba_2V_2O_7$ and $Ba_3(VO_4)_2$ can well coexist at sintering temperatures owing to different crystal structures. The microwave dielectric properties of this system were strongly related to densification, packing fraction, and the volume ratio of $Ba_2V_2O_7$ and $Ba_3(VO_4)_2$. The quality factor $Q \times f$ values and temperature coefficients of the resonant frequency (τ_f) of the ceramics can be significantly boosted by adjusting the relative content of the two phases. Consequently, a high $Q \times f$ value of 71,700 GHz, a near-zero τ_f of −1.4 ppm/°C and a low dielectric constant ε_r of 11.4 were obtained for the $x = 0.42$ sample sintered at a low temperature of 875 °C for 4 h, which are superior to those of several available low-loss dielectrics. In addition, no evidence of chemical reaction between the ceramics and Ag was observed during the cofiring process, suggesting that the as-prepared composite ceramics are suitable for low-permittivity low temperature co-fired ceramic applications.

1. Introduction

Small, light weight, portable and multifunctional electronic components are attracting much attention by virtue of the rapid growth of the wireless communication systems and microwave products in the consumer electronic market. The need for these performances of electronic modules has forced manufacturers to search for new integration, packaging and interconnection technologies. An example of such a technology is low-temperature co-fired ceramic (LTCC) technology, which has been widely utilized in microwave communication systems during the recent years for the benefits they offered in the fabrications of miniature multilayered devices [1,2]. As the research interests are extended to the millimeter-wave range from industrial, scientific, and medical (ISM) bands, a high quality factor ($Q \times f$) together with a low permittivity ε_r tend to play a more prominent role. Furthermore, the LTCC dielectrics should be well sintered below the melting point of the electrode metals, for example, below 961 °C for silver or 1064 °C for copper, and have a near-zero temperature coefficient of the resonant frequency (τ_f) [3,4]. Al_2O_3 ($\varepsilon_r = 9.8$, $Q \times f = 333{,}000$ GHz and $\tau_f = -60$ ppm/°C) [5], $Mg_4Nb_2O_9$ ($\varepsilon_r = 12.4$, $Q \times f = 192{,}268$ GHz and $\tau_f = -70.5$ ppm/°C) [6], Mg_2SiO_4 ($\varepsilon_r = 6.8$, $Q \times f = 241{,}500$ GHz and $\tau_f = -67$ ppm/°C) [7], Zn_2SiO_4 ($\varepsilon_r = 6.6$, $Q \times f = 219{,}000$ GHz and $\tau_f = -61$ ppm/°C) [8], and $Sm_3Ga_5O_{12}$ ($\varepsilon_r = 12.4$, $Q \times f = 192{,}173$ GHz and $\tau_f = -19.2$ ppm/°C) [9] ceramics all exhibited a low ε_r and a giant $Q \times f$ value. However, the large negative τ_f values extremely restricted their immediate commercial applications. Additionally, their sintering temperatures are too high to be used in LTCC multilayer devices. Addition of low melting point oxides or glasses was known to be the cheapest and most effective method for lowering sintering temperature by means of liquid-phase sintering. Unfortunately, the presence of the glassy phase in the sintered ceramics deteriorates the microwave dielectric properties of the matrix ceramics due to its high loss behavior. Therefore, new material systems with excellent microwave dielectric properties and an inherently low sintering temperature need to be developed for LTCC devices [10].

Recently, a few material systems with intrinsically lower sintering temperatures have been intensively investigated as candidates for LTCC technology. Some compounds composed of TeO_2, Bi_2O_3, MoO_3, P_2O_5, LiO_2, and V_2O_5 have gained considerable attention in this context [11–16]. Among them, low-firing vanadate ceramics with light weight, low-cost, easily-processable characteristics such as $Mg_2V_2O_7$ [17], $LiCa_3MgV_3O_{12}$ [18], $Ca_5A_4(VO_4)_6$ (A = Zn, Mg) [11], $Ca_5Co_4(VO_4)_6$ [16], show potential microwave properties and

* Corresponding author. Tel.: +86 551 62905285; fax: +86 551 62905285.
E-mail address: piezolab@hfut.edu.cn (R. Zuo).

http://dx.doi.org/10.1016/j.jallcom.2014.10.056
0925-8388/

exhibit good chemical compatibility with silver during the cofiring process. Joung et al. [17] first reported the microwave properties of $Ba_2V_2O_7$ (ε_r = 10.1, $Q \times f$ = 51,630 GHz and τ_f = −26.5 ppm/°C) sintered at 900 °C, possibly being a good candidate material for LTCC devices if its negative τ_f value can be tailored to be near zero.

In order to achieve a microwave dielectric material with a near-zero τ_f value, the most convenient and promising way is to combine two compounds having negative and positive τ_f values to form a solid solution or mixed phases. According to the mixture rule, it always becomes a trade-off problem when two compounds with opposite τ_f values were mixed, which means the improvement of τ_f value is always based on the sacrifice of $Q \times f$ value. For instance, mixing $MgTiO_3$ (ε_r = 17, $Q \times f$ = 160,000 GHz and τ_f = -50 ppm/°C) and $CaTiO_3$ (ε_r = 170, $Q \times f$ = 3600 GHz and τ_f = 800 ppm/°C) would lead to a compromising combination of dielectric properties (ε_r = 21, $Q \times f$ = 56,000 GHz and τ_f = 0 ppm/°C) for $0.95MgTiO_3$–$0.05CaTiO_3$ [19]. Nevertheless, some novel phenomena such as the $Q \times f$ values of the mixtures were higher than the end phases have appeared in several composite systems, for example, $MgAl_2O_4$–TiO_2 [4], $ZnAl_2O_4$–TiO_2 [20], $BaWO_4$–$Ba_3(VO_4)_2$ [10], $Ba_4LiNb_3O_{12}$–$BaWO_4$ [21]. So far, the mechanism of the enhancement in $Q \times f$ value in these systems is still not distinct because the $Q \times f$ value is usually affected by diverse factors, and it needs to be further studied.

Since the $Ba_2V_2O_7$ ceramics have negative τ_f values, the temperature compensators with positive τ_f values should be added in order to achieve a near-zero τ_f value. As known in BaO–V_2O_5 system, $Ba_3(VO_4)_2$ not only has a large positive τ_f value (52 ppm/°C) and good microwave dielectric properties (ε_r = 14 and $Q \times f$ = 42,000 GHz), but also can be sintered at a relatively low temperature (1100 °C) [22]. And it was often used as a τ_f-tailoring material, such as $Ba_3(VO_4)_2$–Mg_2SiO_4 [22], $Ba_3(VO_4)_2$–$BaWO_4$ [10], $Ba_3(VO_4)_2$–$Zn_{1.87}SiO_{3.87}$ [23], $Ba_3(VO_4)_2$–$LiMg_{0.9}Zn_{0.1}PO_4$ [24]. So, it is logical to speculate that a diphasic microwave dielectric ceramic with a near-zero τ_f value, a desirable $Q \times f$ value and a low sintering temperature would be obtained in BaO–V_2O_5 system by combining $Ba_3(VO_4)_2$ and $Ba_2V_2O_7$. In this work, both $Ba_2V_2O_7$ and $Ba_3(VO_4)_2$ powders were individually synthesized by a conventional mixed-oxide route. $(1-x)Ba_2V_2O_7$–$xBa_3(VO_4)_2$ (x = 0.27–0.52, in volume percent) composite ceramics were prepared for the first time and their microwave dielectric properties were investigated systematically based on the densification, the XRD patterns, and the microstructure analysis. The $Q \times f$ values were particularly discussed from the viewpoint of the packing fraction. In addition, the chemical compatibility between the prepared material and Ag electrode was also studied.

2. Experimental procedure

The starting materials used were high-purity (>99%) powders of analytic-grade $BaCO_3$ and V_2O_5. $Ba_2V_2O_7$ and $Ba_3(VO_4)_2$ powders with stoichiometric compositions were first synthesized individually using a conventional solid-state reaction route by calcining at 750 °C for 4 h and 800 °C for 4 h, respectively. Subsequently, the $(1-x)Ba_2V_2O_7$–$xBa_3(VO_4)_2$ (x = 0.27–0.52, in volume percent) composite powders were ball milled in a nylon jar with zirconia balls on a planetary milling machine (QM-3SP2, NanDa Instrument Plant, Nanjing, China) at 360 rpm for 8 h and alcohol as media. The slurries were dried, granulated with 5 wt% PVA as a binder, and then pressed into cylinders of 10 mm in diameter and 5–6 mm in height via a uniaxial pressure of 100 MPa in a stainless-steel die. These specimens were first heated at 550 °C for 4 h to burn out the organic binder, and then sintered at temperatures from 825 °C to 925 °C for 4 h in air. Moreover, in order to study the chemical compatibility with Ag, the composite powders mixed with 20 wt% Ag powder were ground in an agate mortar, then pressed into disks and sintered at 875 °C for 4 h afterwards.

The crystalline phases of the sintered samples were determined by an X-ray diffractometer (XRD, D/Max2500V, Rigaku, Tokyo, Japan) using Cu Kα radiation. The phase identification, background subtraction, $K\alpha_2$ subtraction, smoothing, and spectrum fitting were carried out by using Jade 6.0 (Jade Software Corporation Limited, Christchurch, New Zealand). The molar volume of each phase in the $(1-x)Ba_2V_2O_7$–$xBa_3(VO_4)_2$ samples was also obtained by using the above software and the cell refinement with a relative error of 4%.

The bulk densities of the sintered samples were measured by the Archimedes method. The microstructural observations of the natural and fractured surface and the quantitative analysis of elements in different grains were performed using a field emission scanning electron microscope (FE-SEM, SU8020, JEOL, Tokyo, Japan) equipped with an energy dispersive spectrometer (EDS). A network analyzer (Agilent, N5230C, Palo Alto, CA) and a temperature chamber (GDW-100, Saiweisi, Changzhou, China) were used to measure the dielectric properties of the well-polished ceramic samples with an aspect ratio of 1.8–2.2, which is ideal for maximum separation of the modes, in the microwave frequency range by means of Hakki–Coleman post resonator method [25]. The dielectric constants were measured using the electric probe of an antenna as suggested by Courtney [26]. The loaded quality factor Q_L was determined using a shielded cavity (Resonant cavity, QWED, Warsaw, Poland) at the TE_{011} mode of resonance, which can be least perturbed by the surrounding field variations. And the dielectric loss ($\tan\delta$) was calculated by using the software provided by the $TE_{01\delta}$-shield cavity supplier, through which the Q values can be obtained in accordance with the equation $Q = 1/\tan\delta$. The τ_f value of the samples was measured by noting the change in the resonant frequency over a temperature range from 25 °C to 80 °C, and it can be calculated by the following equation:

$$\tau_f = \frac{f_2 - f_1}{f_1(T_2 - T_1)} \quad (1)$$

where f_1 and f_2 represent the resonant frequencies at T_1 and T_2, respectively.

3. Results and discussion

3.1. XRD analysis

Fig. 1(a) depicts the normalizing XRD patterns of $(1-x)Ba_2V_2O_7$–$xBa_3(VO_4)_2$ (x = 0–1, in volume fraction) ceramics sintered at 875 °C for 4 h. Compared to the standard patterns, the x = 0 and x = 1 samples can be considered as pure-phase $Ba_2V_2O_7$ (JCPDS #39-1432) and $Ba_3(VO_4)_2$ (JCPDS #29-0211), respectively. For other samples with $0 < x < 1$, all the main diffraction peaks can be well indexed in terms of the standard patterns of $Ba_2V_2O_7$ and $Ba_3(VO_4)_2$. No trace of secondary phases can be observed, indicating that the $Ba_2V_2O_7$ and $Ba_3(VO_4)_2$ can well coexist in the sintered bodies with different x values. This result is consistent with the outcome of the Laser Raman spectrum reported by Unnimaya et al. [27]. The coexistence of $Ba_2V_2O_7$ and $Ba_3(VO_4)_2$ in the sintered bodies might be due in large part to the different crystalline structures of two phases and the different coordinational relations between V^{5+}, Ba^{2+} and O^{2-} in each crystal structure. $Ba_3(VO_4)_2$ is of space group $R\bar{3}2/m$ with a hexagonal structure, in which the V^{5+} ions are located inside tetrahedral $[VO_4]$ units linked by six- and ten-fold coordinated Ba^{2+} ions [28]. On the other hand, $Ba_2V_2O_7$

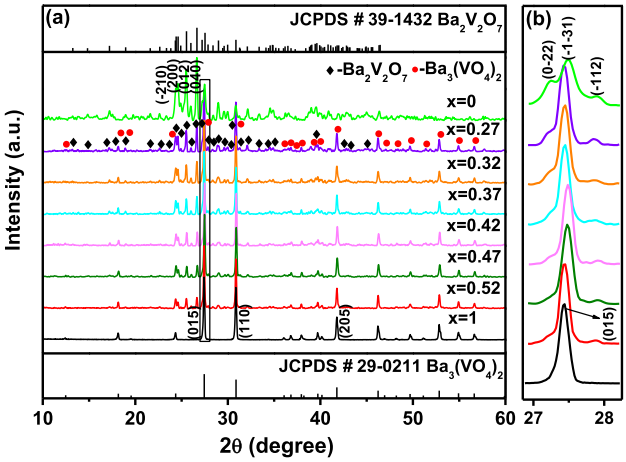

Fig. 1. XRD patterns of $(1-x)Ba_2V_2O_7$–$xBa_3(VO_4)_2$ (x = 0–1) ceramics sintered at 875 °C for 4 h, as compared to the standard patterns of $Ba_2V_2O_7$ and $Ba_3(VO_4)_2$.

is of space group P1 with a triclinic structure, in which two unique divanadate groups formed sheets parallel to (100). And these sheets of divanadate groups are linked by four unique Ba^{2+} ions which lie between themselves [29]. These differences in the crystal structure inhibit the formation of solid solution between $Ba_3(VO_4)_2$ and $Ba_2V_2O_7$. In addition, it can be observed that the intensities of main diffraction peaks of $Ba_2V_2O_7$ such as (040), (012), (200), and (−210). marked in the XRD patterns become weakened obviously with increasing x. However, it is worthwhile to note that the intensities of main diffraction peaks of $Ba_3(VO_4)_2$ such as (015), (110), and (205). exhibit almost no change with varying x values. The crushed powder of the sample with $x = 0.27$ could produce comparably high diffraction intensities of main peaks of $Ba_3(VO_4)_2$ compared to those of the pure $Ba_3(VO_4)_2$ sample ($x = 1$), which has also been observed in other $Ba_3(VO_4)_2$ containing composite ceramics including $Ba_3(VO_4)_2$–Mg_2SiO_4, and $Ba_3(VO_4)_2$–$BaWO_4$ [10,22]. This result may be attributed to the big discrepancy in the crystallizability between $Ba_2V_2O_7$ and $Ba_3(VO_4)_2$, which is consistent with the XRD data of the two pure phases. The diffraction peaks of the pure $Ba_2V_2O_7$ sample ($x = 0$) are relatively broad and have lower intensities. In addition, the enclosed region in Fig. 1(a) was enlarged and as shown in Fig. 1(b), with increasing the $Ba_3(VO_4)_2$ content, the main peaks (0 −2 2), (−1 −3 1), (−1 1 2) of $Ba_2V_2O_7$ phase and (0 1 5) of $Ba_3(VO_4)_2$ phase firstly shifted toward higher angle and then shifted toward lower angle again. To understand the unusual change with more details, the unit cell volume (V_{unit}) of each phase was calculated based on cell refinement and presented in Table 1. It can be found that V_{unit} of each phase gradually decreased with increasing $Ba_3(VO_4)_2$ content and both reached a minimum value at $x = 0.42$ compositions, then increased with further increasing $Ba_3(VO_4)_2$ content. This unusual variation in cell volume has also been found in other vanadates and reasonably explained by the presence of V^{4+} [16]. Thus we speculated that the anomalous change on V_{unit} may be connected the change in the valence states of V atoms and we will give a detail analysis in our future work.

Fig. 2 illustrates the effect of sintering temperature and duration on the phase structure of $0.58Ba_2V_2O_7$–$0.42Ba_3(VO_4)_2$ ceramics, in which the XRD pattern of the 20 wt% Ag-added $x = 0.42$ ceramic sample cofired at 875 °C for 4 h was also given for comparison. On the one hand, there is still no apparent secondary phase to be observed in the case of changing sintering time, suggesting that the coexistence of the two phases in the $x = 0.42$ ceramic is stable at 875 °C. This result reveals that the sintering time may exert an influence on the sample densities, while does not play an obvious role in inducing any chemical reaction between $Ba_2V_2O_7$ and $Ba_3(VO_4)_2$. On the other hand, it can be found that all diffraction peaks slightly shift toward higher angles as the sintering temperature increases from 825 °C to 925 °C for the $x = 0.42$ ceramic. According to the XRD patterns, the V_{unit} obtained by the cell refinement of the two phases shrinks from 177.93 Å^3/mol to 177.00 Å^3/mol for $Ba_2V_2O_7$, and 204.91 Å^3/mol to 204.05 Å^3/mol for $Ba_3(VO_4)_2$ respectively, which may be caused by the V_2O_5 evaporation during sintering process. A similar decrease of lattice parameter in $Ca_5Co_4(VO_4)_6$ ceramics related to V-evaporation was also reported by Liu et al. [16]. In addition, it can be also found that the crystallizability of $Ba_2V_2O_7$ is enhanced as sintering temperature increases in spite of an unobvious tendency, but is not affected by sintering duration time. Moreover, for the cofired sample of the $x = 0.42$ composition

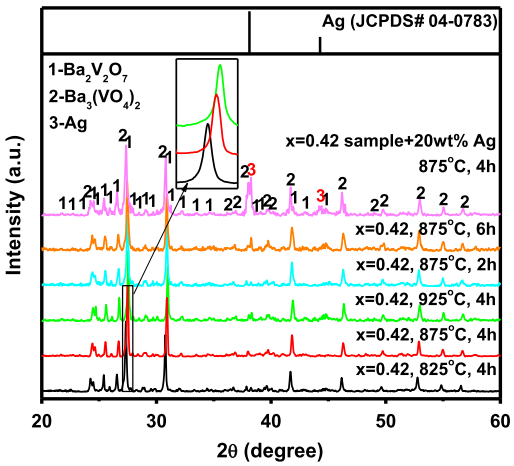

Fig. 2. XRD patterns of $0.58Ba_2V_2O_7$–$0.42Ba_3(VO_4)_2$ ceramics sintered at various temperatures for 4 h and at 875 °C for different hours and of the 20 wt% Ag added $x = 0.42$ ceramic sample cofired at 875 °C for 4 h.

and 20 wt% Ag powder, no additional peaks are present in the XRD pattern other than diffraction peaks of the ceramic sample and Ag (JCPDS #04-0783), implying that $0.58Ba_2V_2O_7$–$0.42Ba_3(VO_4)_2$ ceramic does not react with Ag at the sintering temperature.

3.2. Microstructures

In order to clarify the relationship between the composition and the morphological changes in the samples, the microstructure of the $(1-x)Ba_2V_2O_7$–$xBa_3(VO_4)_2$ ($x = 0.27$–0.52) ceramics sintered at 875 °C for 4 h was observed, as shown in Fig. 3. In general, both $Ba_2V_2O_7$ and $Ba_3(VO_4)_2$ grains usually grow into pebble-like in monophasic or composite ceramics [10,17,22–24]. Thus, it is hard to distinguish the two phases from the morphology. Nevertheless, the result of EDS analysis (Fig. 3(f)) shows that the rod-like grains (marked 1 in Fig. 3(c)) contain Ba, V and O elements in an approximate molar ratio of Ba:V:O = 2:2:7, and the pebble-like grains (marked 2 in Fig. 3(c)) are totally composed of the same elements but with a different molar ratio of Ba:V:O = 3:2:8, which can basically confirm the identification of each kind of grains in the microstructure. This result suggests that the addition of $Ba_3(VO_4)_2$ to some extent boosts the partial grains of $Ba_2V_2O_7$ to grow along a differential direction, resulting in the rod-like morphology of $Ba_2V_2O_7$ grains. And the variation of the composition does not cause a significant difference in the grain size of the two phases. In addition, it can be believed that the ionic diffusion of Ba^{2+} and V^{5+} occurred during the sintering process and slightly changed the molar ratio of elements of each phase in the composite, which might have an influence on the dielectric properties of each phase in the composite ceramics. On the other hand, the effects of the sintering temperature on the microstructure of $0.58Ba_2V_2O_7$–$0.42Ba_3(VO_4)_2$ ceramics are demonstrated in Fig. 4. It can be observed that remaining pores are visible in the ceramics sintered at 825 °C, and the densification rapidly increases as the sintering temperature surpasses 850 °C. However, the grain abnormal growth and nonuniformity can be simultaneously promoted. The enhanced grain growth behavior tends to lower the sintering driving force for densification and inhibit extraction of pores from

Table 1
The unit cell volume (V_{unit}) of each phase in $(1-x)Ba_2V_2O_7$–$xBa_3(VO_4)_2$ ($x = 0.27$–0.52) ceramics sintered at 875 °C for 4 h.

V_{unit} (Å)	$x = 0$	$x = 0.27$	$x = 0.32$	$x = 0.37$	$x = 0.42$	$x = 0.47$	$x = 0.52$	$x = 1$
$Ba_2V_2O_7$	179.80	179.70	179.67	179.60	177.93	178.60	178.83	
$Ba_3(VO_4)_2$		206.08	205.90	205.86	204.91	205.47	205.92	206.11

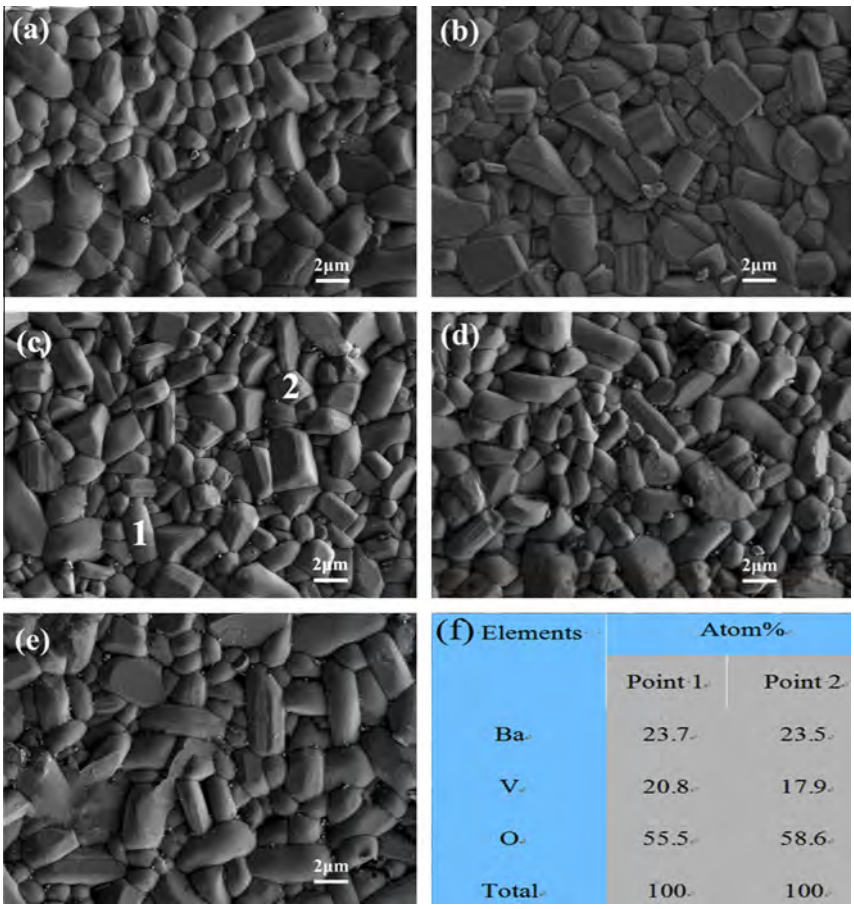

Fig. 3. SEM photographs of $(1-x)Ba_2V_2O_7$–$xBa_3(VO_4)_2$ ceramics sintered at 875 °C for 4 h: (a) x = 0.27, (b) x = 0.37, (c) x = 0.42, (d) x = 0.47, (e) x = 0.52 and (f) EDS result for the x = 0.42 sample sintered at 875 °C for 4 h.

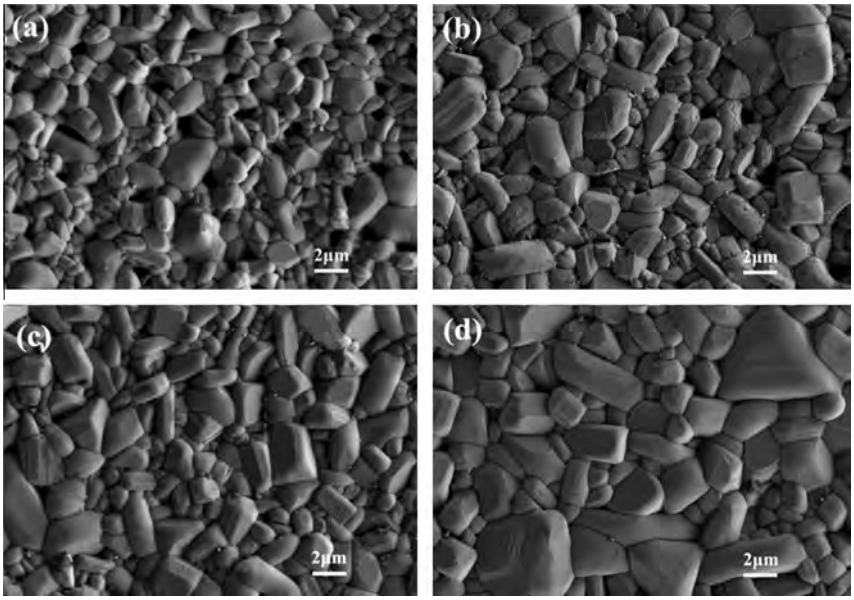

Fig. 4. SEM photographs of $0.58Ba_2V_2O_7$–$0.42Ba_3(VO_4)_2$ ceramics sintered at various temperatures for 4 h: (a) 825 °C, (b) 850 °C, (c) 875 °C and (d) 925 °C.

green bodies, so that the sample density decreases as the sintering temperature is too high. As a result, samples sintered at 875 °C have a relatively high density without obvious porosity and exhibit a uniform microstructure.

3.3. Relative density and microwave dielectric properties

Fig. 5 represents the relative densities, ε_r, and $Q \times f$ values of $(1-x)Ba_2V_2O_7$–$xBa_3(VO_4)_2$ (x = 0.27–0.52) ceramics as a function

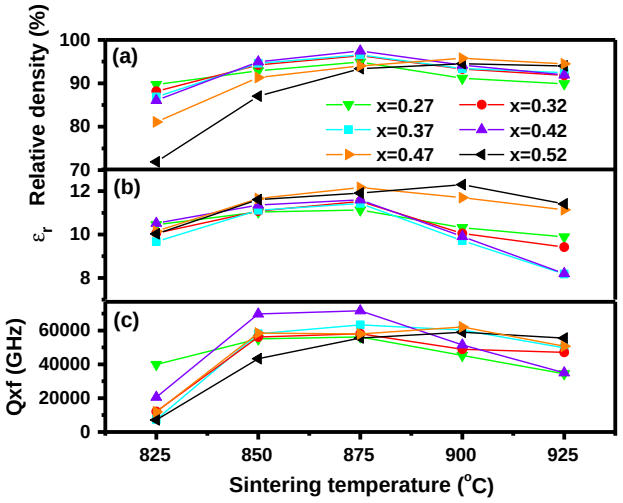

Fig. 5. (a) Relative densities, (b) ε_r and (c) $Q \times f$ values of $(1-x)Ba_2V_2O_7$–$xBa_3(VO_4)_2$ (x = 0.27–0.52) ceramics as a function of sintering temperature.

of the sintering temperature. The relative densities in percentage stand for the ratios of the measured densities to the theoretical densities. The theoretical densities of the composite samples were roughly evaluated by the following equation:

$$\rho = \frac{\omega_1 + \omega_2}{\omega_1/\rho_1 + \omega_2/\rho_2} \quad (2)$$

where ω_1 and ω_2 are the weight fractions of $Ba_2V_2O_7$ and $Ba_3(VO_4)_2$, respectively; ρ_1 and ρ_2 are the theoretical densities of $Ba_2V_2O_7$ and $Ba_3(VO_4)_2$, respectively. Since the unit cell volume of $Ba_2V_2O_7$ and $Ba_3(VO_4)_2$ changed with varied x, the ρ_1 and ρ_2 should be calculated by using the Eq. (3):

$$\rho = \frac{ZM}{N_A V_{\text{unit}}} \quad (3)$$

where Z is the number of atoms per unit cell, M is the molar weight (g/mol), N_A is the Avogadro number (6.023×10^{23} atoms per mol), and V_{unit} is the volume of the unit cell (in cm^3) [6]. For all samples, with increasing the sintering temperature, the relative densities increase to a maximum value and decline thereafter. It can be seen from Fig. 5(a) that the maximum densities of approximately 96.5% were achieved in the temperature range of 850–875 °C for the composite samples with $x \leqslant 0.42$, which agrees well with the microstructural observation of the samples (Fig. 3(a–c)), and in the temperature range of 900–925 °C for the $x \geqslant 0.47$. It is also evident that the densities decrease with increasing x value at a low temperature range below 875 °C. These results may be due to the relatively high densification temperature of $Ba_3(VO_4)_2$ (1100 °C) compared with $Ba_2V_2O_7$ (900 °C). The microwave dielectric properties of $(1-x)Ba_2V_2O_7$–$xBa_3(VO_4)_2$ ceramics with respect to sintering temperatures are shown in Fig. 5(b and c). It is obvious that the ε_r and $Q \times f$ values change with the sintering temperature in a manner similar to that of the density, as the ε_r and $Q \times f$ values are usually strongly dependent on density. The ε_r value increases from 11 to 12.3 with increasing x, which is mainly attributed to a larger ε_r value of $Ba_3(VO_4)_2$ than that of $Ba_2V_2O_7$. From the variation of $Q \times f$ values against sintering temperature, it can be observed that the optimized sintering temperature of the samples with $x \leqslant 0.42$ is 875 °C, while 900 °C for the samples with $x \geqslant 0.47$. For a given x, the increase of the ε_r and $Q \times f$ value is initially due to the increase of density, which implies that the densification of the ceramics plays an important role in controlling the dielectric loss and the same phenomenon has also been shown for other microwave dielectric materials [16,22–24]. A further increase in sintering temperature results in a rapid grain growth and an appearance of pores as observed in Fig. 4(d), and consequently leads to the reduction of the ε_r and $Q \times f$ value. Moreover, the effects of the sintering duration on the relative density and microwave dielectric properties of the $0.58Ba_2V_2O_7$–$0.42Ba_3(VO_4)_2$ ceramics also have been investigated by sintering the samples at 875 °C for different hours, as shown in Fig. 6. It can be observed that the ε_r and $Q \times f$ values of the ceramics varying with the sintering duration also show a similar tendency to the sample density (see the inset of Fig. 6), and both reach a maximum value for 4 h. This result may be ascribed to the fact that still no secondary phases appear with changing the sintering time (Fig. 2), and the maximum sample density has been almost reached after 4 h.

The microwave dielectric properties of $(1-x)Ba_2V_2O_7$–$xBa_3(VO_4)_2$ ceramics sintered at optimized sintering temperatures are shown in Fig. 7. With x increasing from 0.27 to 0.52, both ε_r and τ_f values increase gradually, while the $Q \times f$ values first increase to a maximum value of 71,700 GHz at x = 0.42 and drop down subsequently. It is evident that the microwave dielectric properties of the composite ceramics are obviously related to the change of the $Ba_3(VO_4)_2$ content in the mixtures. The well-known empirical model for multiphase ceramics was used to verify the above results. The calculated ε_r, $Q \times f$, and τ_f values of different samples were obtained by the following equations [23]:

$$\varepsilon_r^{\alpha} = V_1 \varepsilon_{r1}^{\alpha} + V_2 \varepsilon_{r2}^{\alpha} \quad (4)$$

$$\frac{1}{Qf} = \frac{V_1}{Qf} + \frac{V_2}{Qf} \quad (5)$$

$$\tau_f = V_1 \tau_{f1} + V_2 \tau_{f2} \quad (6)$$

where V is the volume fraction of each phase. The subscripts 1 and 2 stand for $Ba_2V_2O_7$ and $Ba_3(VO_4)_2$ phases, respectively, and α is a constant which depends on the type of the mixing rule: α = 1, −1 and 0 represent serial, parallel and logarithmic mixing model, respectively. From Fig. 7, it can be found that the experimentally measured results of ε_r and τ_f values are in agreement with the calculated results in terms of the change trend with x. However, a certain deviation between the experimental and the calculated results was clearly observed, which was also found in other works [21–23]. This may be due to the following reasons. Firstly, the distribution of different phases is not perfectly uniform as manifested in Fig. 3(c), where the rod-like ($Ba_2V_2O_7$) and the pebble-like ($Ba_3(VO_4)_2$) grains arranged randomly; secondly, the microwave dielectric properties of each phase may be different in the mixtures from those in the monophasic ceramics owing to the diffusion of different atoms; thirdly, the discrepancy of the crystallizability between the two phases in the composite ceramics exists to a certain extent; and

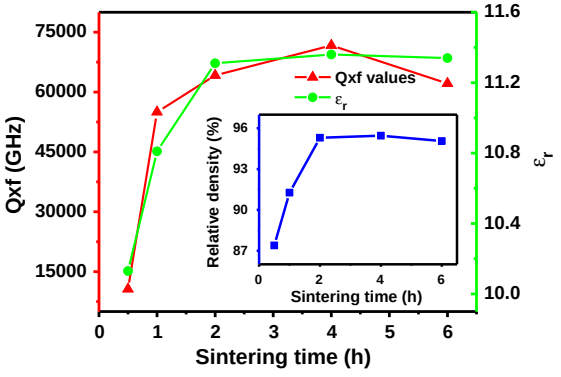

Fig. 6. Relative densities, ε_r and $Q \times f$ values of $0.58Ba_2V_2O_7$–$0.42Ba_3(VO_4)_2$ ceramics sintered at 875 °C for different sintering duration time.

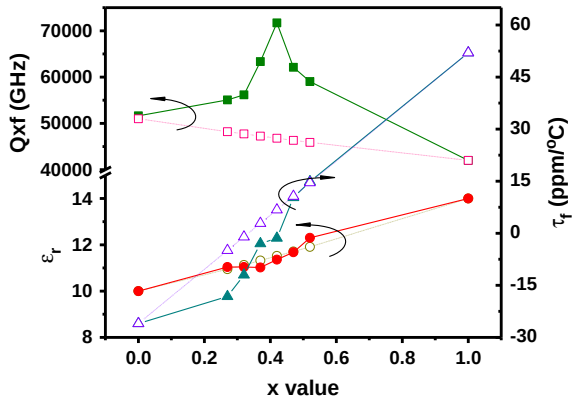

Fig. 7. The calculated (hollow symbols) and measured (solid symbols) microwave dielectric properties of $(1-x)Ba_2V_2O_7$–$xBa_3(VO_4)_2$ (x = 0.27–0.52) ceramics sintered at optimized sintering temperatures (875 °C for the samples with $x \leqslant 0.42$, and 900 °C for $x \geqslant 0.47$) for 4 h.

finally, the uncertainty of the calculated volume fraction is unavoidable [30]. Furthermore, it is probably worthwhile to note that the $Q \times f$ value, which depends considerably on diverse factors such as synthesizing conditions, purity of the chemicals, lattice defects, internal stress, cation ordering and crystallizability [24], does not follow any mixture rule in the entire compositional range. Since the relative densities of the samples are all above 95% (Fig. 5(a)) and no secondary phases (Fig. 1(a)) and no significant change in grain size (Fig. 3) were observed, the extrinsic effects from the porosity, secondary phases and grain size on the difference of the $Q \times f$ value could be generally neglected [31]. Kim et al. reported that the $Q \times f$ value increased with the increase of packing fraction by virtue of the decrease of lattice vibrations [32]. In the present investigation, the high $Q \times f$ values of the composite ceramics might be closely related to the packing fractions of each phase in the diphasic structure, which have been calculated using the relation given by:

$$\text{Packing fraction } (\%) = \frac{\text{volume of packed ions}}{\text{volume of unit cell}} \times Z \qquad (7)$$

where Z is the number of formula units per unit cell of the compound. The results are shown in Fig. 8. It can be observed that the $Q \times f$ value increased from 55,070 to 71,700 GHz, and packing fractions range from 57.9% to 58.5% for $Ba_2V_2O_7$ phase and 64.3% to 64.7% for $Ba_3(VO_4)_2$ phase. The results manifest that the variation of $Q \times f$ value was consistent with that of packing fraction of each phase in the composite ceramics. The increase in packing fraction

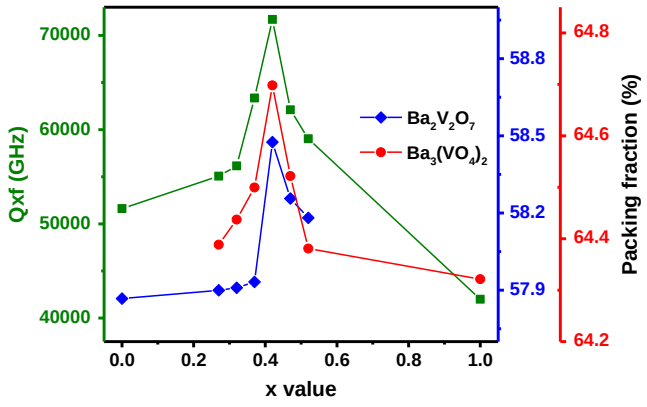

Fig. 8. The $Q \times f$ values and packing fractions of $(1-x)Ba_2V_2O_7$–$xBa_3(VO_4)_2$ (x = 0.27–0.52) ceramics sintered at optimized temperatures.

means a decreased vibration space, and this in turn may give rise to a decrease in anharmonic vibration of atoms. Consequently, the increase in $Q \times f$ value would be attributed primarily to the increase in packing fraction.

4. Conclusion

The novel microwave dielectric composite ceramics were successfully prepared by cofiring the mixed-powder compacts of $Ba_2V_2O_7$ and $Ba_3(VO_4)_2$. The phase structure, densification behavior, microstructure and microwave dielectric properties were investigated systematically based on the sintering temperature and duration time, and the relative content of each phase. Higher packing fraction of each phase resulting from appropriate relative content of the two phases in the sintered samples significantly improves the $Q \times f$ value. Several factors such as element inter-diffusion and big discrepancy of the crystallizability between the two phases make the experimentally measured properties deviate from the calculated ones although the change tendency of the properties with the fraction of each phase is generally consistent. The experimental results demonstrate that the diphasic ceramics with 42% $Ba_3(VO_4)_2$ can be well sintered at 875 °C and exhibit excellent microwave dielectric properties of ε_r = 11.4, $Q \times f$ = 71,700 GHz, τ_f = −1.4 ppm/°C and good chemical compatibility with Ag, which possibly make them become an ideal candidate for low-permittivity LTCC applications for microwave components.

Acknowledgement

Financial support from the National Natural Science Foundation of China (Grant Nos. 51272060 and 51472069) is gratefully acknowledged.

References

[1] H.F. Zhou, X.L. Chen, L. Fang, X.B. Liu, Y.L. Wang, J. Am. Ceram. Soc. 93 (2010) 3976–3979.
[2] W. Lei, W.Z. Lu, D. Liu, J.H. Zhu, J. Am. Ceram. Soc. 92 (2009) 105–109.
[3] J.J. Xue, S.P. Wu, J.H. Li, J. Am. Ceram. Soc. 96 (2013) 2481–2485.
[4] K.P. Surendran, P.V. Bijumon, P. Mohanan, M.T. Sebastian, Appl. Phys. A 81 (2005) 823–826.
[5] N. Mc, N. Alford, S.J. Penn, J. Appl. Phys. 80 (1996) 5895–5898.
[6] A. Yoshida, H. Ogawa, A. Kan, S. Ishihara, Y. Higashida, J. Eur. Ceram. Soc. 24 (2004) 1765–1768.
[7] T. Tsunooka, M. Androu, Y. Higashida, H. Sugiura, H. Ohsato, J. Eur. Ceram. Soc. 23 (2003) 2573–2578.
[8] Y.P. Guo, H. Ohsato, K. Kakimoto, J. Eur. Ceram. Soc. 26 (2006) 1827–1830.
[9] J.C. Kim, M.H. Kim, S. Nahm, J.H. Paik, J.H. Kim, H.J. Lee, J. Eur. Ceram. Soc. 27 (2007) 2865–2870.
[10] H. Zhuang, Z.X. Yue, S.Q. Meng, F. Zhao, L.T. Li, J. Am. Ceram. Soc. 91 (2008) 3738–3741.
[11] G.G. Yao, P. Liu, H.W. Zhang, J. Am. Ceram. Soc. 96 (2013) 1691–1693.
[12] D. Zhou, L.X. Pang, H. Wang, X. Yao, J. Eur. Ceram. Soc. 31 (2011) 2749–2752.
[13] D. Zhou, C.A. Randall, H. Wang, X. Yao, J. Am. Ceram. Soc. 94 (2011) 348–350.
[14] R. Umemura, H. Ogawa, H. Ohsato, A. Kana, A. Yokoi, J. Eur. Ceram. Soc. 25 (2005) 2865–2870.
[15] D. Zhou, H. Wang, L.X. Pang, C.A. Randall, X. Yao, J. Am. Ceram. Soc. 92 (2009) 2242–2246.
[16] G.G. Yao, P. Liu, X.G. Zhao, J.P. Zhou, H.W. Zhang, J. Eur. Ceram. Soc., doi:http://dx.doi.org/10.1016/j.jeurceramsoc.2014.03.026.
[17] M.R. Joung, J.S. Kim, M.E. Song, S. Nahm, J. Am. Ceram. Soc. 92 (2009) 3092–3094.
[18] L. Fang, C.X. Su, H.F. Zhou, Z.H. Wei, H. Zhang, J. Am. Ceram. Soc. 96 (2013) 688–690.
[19] K. Wakino, Ferroelectrics 91 (1989) 69–86.
[20] C.L. Huang, T.J. Yang, C.C. Huang, J. Am. Ceram. Soc. 92 (2009) 119–124.
[21] C. Tian, Z.X. Yue, Y.Y. Zhou, Mater. Sci. Eng., B 178 (2013) 178–182.
[22] S.Q. Meng, Z.X. Yue, H. Zhuang, F. Zhao, L.T. Li, J. Am. Ceram. Soc. 93 (2010) 359–361.
[23] Y. Lv, R.Z. Zuo, Z.X. Yue, Mater. Res. Bull. 48 (2013) 2011–2017.
[24] Y. Lv, R.Z. Zuo, Y. Cheng, C. Zhang, J. Am. Ceram. Soc. 96 (2013) 3862–3867.
[25] B.W. Hakki, P.D. Coleman, IEEE Trans. Microwave Theory Tech. 8 (1960) 402–410.
[26] W.E. Courtney, IEEE Trans. Microwave Theory Tech. 18 (1970) 476–485.

[27] A.N. Unnimaya, E.K. Suresh, J. Dhanya, R. Ratheesh, J. Mater. Sci. 25 (2014) 1127–1131.
[28] M.H. Whitmore, H.R. Verdun, D.J. Singel, Phys. Rev. B 47 (1993) 11479–11482.
[29] F.C. Hawthorne, C. Calvo, J. Solid State Chem. 26 (1978) 345–355.
[30] M.Z. Dong, Z.X. Yue, H. Zhuang, S.Q. Meng, L.T. Li, J. Am. Ceram. Soc. 91 (2008) 3981–3985.
[31] H. Zhuang, Z.X. Yue, F. Zhao, L.T. Li, J. Am. Ceram. Soc. 91 (2008) 3275–3279.
[32] E.S. Kim, C.J. Jeon, P.G. Clem, J. Eur. Ceram. Soc. 30 (2010) 1731–1736.